Catalysis Today 144 (2009) 160–165

Contents lists available at ScienceDirect

Catalysis Today

journal homepage: www.elsevier.com/locate/cattod

Photocatalysis on silver-layer silicate/titanium dioxide composite thin films at solid/vapour interface

Judit Ménesi [a], Renáta Kékesi [a], Albert Oszkó [a], Volker Zöllmer [b], Torben Seemann [b], André Richardt [c], Imre Dékány [a,*]

[a] Department of Physical Chemistry and Material Science and Suparmolecular and Nanostructured Materials Research Group of Hungarian Academy of Sciences, University of Szeged, H-6720 Szeged, Aradi Vertanuk tere 1, Hungary
[b] Fraunhofer-Institute for Manufacturing and Advanced Materials – IFAM, Wiener Straße 12, D-28359 Bremen, Germany
[c] German Armed Forces Scientific Institute for Protection Technologies – NBC-Protection, P.O. Box 1142, D-29623 Munster, Germany

ARTICLE INFO

Keywords:
Titania-clay composites
Silver-montmorillonite
Photocatalysis
Layer silicates

ABSTRACT

Silver-montmorillonite/TiO_2 composites were prepared using various mixing ratios. The optical properties of the catalyst composites were evaluated DR-UV–vis spectrophotometry. Their photocatalytic efficiencies were tested in the degradation of ethanol vapour at a relative humidity of ~70% in a closed circulating reactor. Light sources used were 15 W lamps, one rich in UV ($\lambda \geq 254$ nm) and one emitting visible light ($\lambda \geq 435$ nm). The course of photodegradation of ethanol vapour was monitored by gas chromatography. By incorporating silver ions into clay minerals/TiO_2 mixtures with different ratio, we obtained composites capable of degrading ethanol in the visible wavelength range about twice as fast as the reference photocatalyst, type P25. The synergistic effect is interpreted as the result of the excellent adsorption capabilities of layer silicates combined with the advantageous effect of silver nanoparticles and silver oxides on light absorption in the visible range.

1. Introduction

The preparation of semiconductor oxide thin films (TiO_2, ZnO and SnO_2) [1] and the analysis of their photocatalytic efficiency represent an important possibility for the utilization of solar energy [2–9]. As the excitation threshold energy of the titanium dioxide is 3.2 eV (λ = 387 nm), it is necessary to use high-energy UV light for the excitation of TiO_2 nanoparticles. It has been reported in many publications that photon absorption on the surface of photocatalysts in the visible range can be increased by incorporation of metal ions (second-generation photocatalysts) [10–16]. Hamal and Klabunde synthesized titanium dioxide doped by silver, carbon and sulphur (Ag/C–S–TiO_2) [17]. They compared the photocatalytic activity of the silver-doped composite with that of the reference, Degussa P25 TiO_2, in gas-phase degradation of acetaldehyde. When using a UV light source (320 nm $< \lambda >$ 420 nm), P25 TiO_2 proved to be more efficient, whereas in the case of a visible light source ($\lambda >$ 420 nm) nm) silver-doped TiO_2 was found to surpass the reference in efficiency. It was established that the shift in the excitation wavelength of the catalyst towards the visible range is due to silver doping. The same result was arrived at by Seery et al., who studied the degradation of the dye rhodamine 6G using a light source with a sun-like spectrum [18]. Incorporation of metal ions into the crystalline structure of TiO_2, however, does not always enhance photocatalytic activity [19] and the stability of the suspension may also decrease due to aggregation, hindering practical utilization in suspension [20].

Another field of this type of research is generation of semiconductor metal oxides on the surface of catalyst supports [21–23]. Supports with large specific surface areas such as layer silicates are capable of accelerating photooxidative processes and they form stable composites. According to Kun et al. [24] the increased adsorption ability is due to the large specific surface area of the clay mineral and to the interlamellar incorporation of TiO_2 particles [25,26]. This phenomenon is termed the synergistic effect of layer silicates, which is responsible for the enhanced activity of TiO_2 nanoparticles in composites as compared to pure TiO_2.

Liu et al. prepared an Ag–TiO_2/montmorillonite composite powder and compared its structure and photocatalytic activity to that of P25 TiO_2, montmorillonite and TiO_2/montmorillonite [27]. They studied the photocatalytic activities of the composites under UV irradiation in the degradation of methylene blue, in aquatic suspension at solid/liquid phase. They found that the Ag–TiO_2/montmorillonite composite with large specific surface area was more efficient in degrading methylene blue than was P25 TiO_2 photocatalyst.

* Corresponding author. Tel.: +36 62 544210; fax: +36 62 544042.
E-mail address: i.dekany@chem.u-szeged.hu (I. Dékány).

0920-5861/$ – see front matter © 2009 Published by Elsevier B.V.
doi:10.1016/j.cattod.2009.02.030

Our objective was to increase the photooxidative degradation rate of ethanol vapour by creating the most efficient TiO_2 photocatalyst/clay composites. To this end the clay mineral, (sodium-montmorillonite) was exchanged by silver cations in aquatic suspension. The catalysts obtained, exhibiting novel optical and structural properties were characterized by various physical methods. For photocatalytic experiments thin films (ca. 1 μm) were prepared from the nanocomposites using "spray coating" technology on a quartz glass cylinder surface in the photoreactor. We studied the degradation of ethanol vapour at the solid/gas interface at ~70% humidity in closed circulating system, in the presence of UV-rich ($\lambda \geq 254$ nm) and visible ($\lambda \geq 435$ nm) light sources.

2. Experimental

2.1. Sample preparation

We used TiO_2 Typ P25 (Evonik, former Degussa AG) and the fine fraction of Na-montmorillonite EXM-838 as layer silicate ($d < 2$ μm, Süd-Chemie AG, Germany) for composite powder preparation. The clay mineral was exchanged with silver nitrate in aquatic suspension (1 mmol g^{-1} clay). The schematic pictures of the structure of the Ag-clay/TiO_2 powder mixture composite have been presented in an earlier publication [28]. The compositions of the catalysts – prepared for thin film using spray coating technique on the glass cylinder was ~1 μm thick – were the following: 20/80, 35/65, 50/50 and 75/25 Ag-clay/TiO_2 ratio.

2.2. Sample characterization

Diode array spectrophotometer (Ocean Optics Inc.) equipped with an integrated sphere was used to record the diffuse reflectance spectra (DRS) of the samples. The optical properties of Ag-ion-exchanged clay/titania catalysts compositions are listed in Table 1.

The specific surface area and the porosity of Ag-clay/TiO_2 nanocomposites were determined by a Micromeritics gas adsorption analyzer (Gemini Type 2375) at 77 K in liquid nitrogen. The structural properties of samples were also characterized by XRD experiments. We can establish that only the disoriented (delaminated) silicate layer structure exists and no intercalation with TiO_2 occurs in the composite. (See schematic picture in Fig. 3.)

X-ray photoelectron (XP) spectra were taken with a SPECS instrument equipped with a PHOIBOS 150 MCD 9 hemispherical electron energy analyzer operated in the FAT mode. The excitation source was the non-monochromatic Kα radiation of a magnesium anode ($h\nu$ = 1253.6 eV). The X-ray gun was operated at 250 W power (12 kV, 14 mA). For data acquisition and evaluation both manufacturer's (SpecsLab2) and commercial (CasaXPS, Origin) software were used.

Photooxidation of ethanol vapour was performed in a reactor (volume: ca. 700 ml) at 25 ± 0.1 °C. The experimental setup and schematic drawing of the photoreactor are described in our previous paper [28,29]. The light sources of the reactor were two types of 15 W low pressure mercury lamp (LightTech, Hungary) as "light source 1" with characteristic emission wavelength at λ_{max} = 254 nm and "light source 2" with characteristic emission wavelength at λ_{max} = 435 nm. The catalyst was sprayed onto the outer side of the inner quartz tube from 10 to 20% aqueous dispersion under N_2 stream. The surface of the catalyst film on the tube wall was 44.8 cm^2, and the coating density was 0.28 ± 0.02 mg cm^{-2}. The film thickness was ca. 0.7–1.0 μm. The reactor was filled with dry synthetic air ($[H_2O] < 5$ ppm) to a final pressure of 760 Torr. After delivery of ethanol and water vapour, the system was left to stand for 30 min for the establishment of the adsorption equilibrium on the catalyst surface. The composition of the vapour phase was analyzed in a gas chromatograph (Shimadzu GC-14B) equipped with a thermal conductivity (TCD) and a flame ionization detector (FID). The flow rate of the gas mixture in the measuring system was 375 cm^3 min^{-1}. The initial concentration of ethanol was 0.25 mol m^{-3} at relative humidity of ~70%.

3. Results

3.1. The specific surface areas and the porosities of the catalysts

For characterization of the catalyst composites we have measured the N_2 adsorption at 77 K. The N_2 adsorption isotherms exhibit adsorption hysteresis. The pore size distribution function was determined from the appropriate region of desorption branch after recording the isotherm, using the Barrett–Joyner–Halenda (BJH) method [30]. This effect show a pore system and the average diameter of whose pores varies between d = 3–4 nm. The specific surface area nearly constant (43–50 m^2 g^{-1}), but the surface area of micropores (a_{mp}) and the volume of the pores are increasing with higher montmorillonite content in the composite catalyst. This data are characteristic only for the surface properties of the powder catalyst samples, but not for the prepared films. However this data show that the presence of the layer silicate in the catalyst give the possibility for adsorption and incorporation of the ethanol and water molecules under the catalytic process. It is well known the swelling properties of clay minerals in aquatic environment, because in the interlayer space there are huge internal surfaces for adsorption of small polar molecules [33].

3.2. Diffuse reflection spectrophotometric studies

Titanium dioxide composite thin films were subjected to diffuse reflection measurements in a diode array spectrophotometer that yields information on the excitability of TiO_2 particles. The DR spectra obtained are shown in Fig. 1. Silver ion content is seen to bring about an increased absorbance in the visible wavelength range (λ = 450–650 nm). The Ag-clay/TiO_2 samples have a broadened absorbance peak maximum at 465 nm (E_g = 2.66 eV) in the visible range, indicated by the brown color of the powder samples. The excitation energy of Degussa P25 TiO_2 is well-known from the literature: E_g = 3.2 eV (λ_g = 387 nm). The optical characteristics of Ag-clay/TiO_2 composites are summarized in Table 1.

3.3. Chemical (XPS) analyses

The XP spectra of O 1s and Ag 3d regions of Na-montmorillonite, TiO_2 (P25), the ion-exchanged montmorillonites and the composites are shown in Fig. 2. The values obtained are normalized to the

Table 1
Structural and optical characteristics of Ag-clay/TiO_2 composite samples.

	Metal content (wt%)	a^s_{BET} (m^2/g)	a^s_{mp} (m^2/g)	V_{mp} ($\times 10^{-3}$ cm^3/g)	d (nm)	λ_g (nm)	E_g (eV)
Ag-clay/TiO_2 20/80	2.16	49.5	0.44	-	3.5	402	3.08
Ag-clay/TiO_2 35/65	3.78	48.0	0.94	0.09	3.5	400	3.10
Ag-clay/TiO_2 50/50	5.40	50.9	3.84	1.63	3.6	397	3.12
Ag-clay/TiO_2 75/25	8.93	43.0	1.57	0.47	3.4	387	3.20

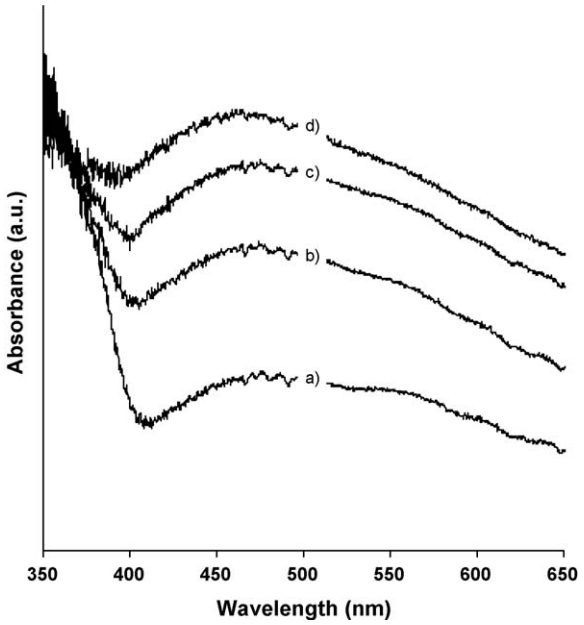

Fig. 1. Diffuse reflectance UV–vis spectra of different Ag-clay/TiO_2 composites: (a) Ag-clay/TiO_2 20/80, (b) Ag-clay/TiO_2 35/65, (c) Ag-clay/TiO_2 50/50 and (d) Ag-clay/TiO_2 75/25.

Table 2
Surface composition of pure and Ag-clay/TiO_2 catalyst samples.

	Atomic concentration (%)					
	Ti	O	Ag	Si	Al	C
Na-montmorillonite	–	62.02	–	22.97	8.30	3.19
TiO_2 (P25)	27.99	60.87	–	–	–	11.14
Ag-clay	–	61.88	1.27	25.27	7.77	3.81
Ag-clay/TiO_2 50/50	8.70	61.14	1.08	16.54	5.81	6.73

binding energy of external carbon (285.1 eV). The samples were measured before as well as after photocatalysis, in order to investigate changes brought by irradiation under 70% humidity. The surface compositions of the samples are summarized in Table 2. The spectra of montmorillonites reveal (Fig. 2a) that when Na-ions are exchanged for Ag-ions, the binding energy of oxygen (E_b = 532.7 eV) is shifted towards higher energies (E_b = 534.5 eV) and its intensity is also slightly increased. As a result of silver addition, the binding energies of the Ti 2p doublets of titanium dioxide and their intensities are altered, which is in good agreement with the results reported by Zhang et al. [31]. These authors found that the intensities of the peaks corresponding to the Ti orbits were increased by the incorporation of Ag-ions. The binding energy of the reference sample (P25 TiO_2) is E_b = 458.7 eV. In the case of the silver-containing sample a shift by about ~0.4 eV

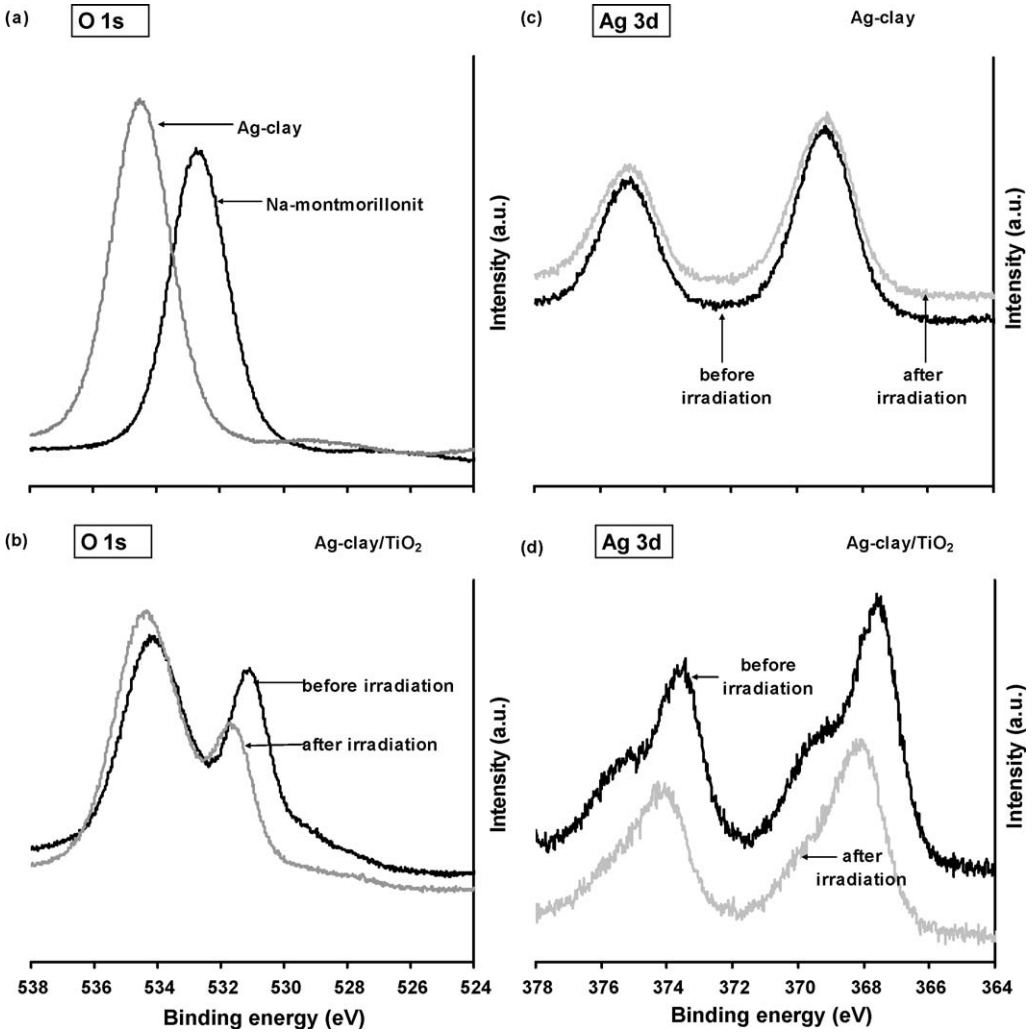

Fig. 2. (a) XP spectra of the O 1s regions of Na-montmorillonite and ion-exchanged montmorillonite clay, (b) O 1s regions of Ag-clay/TiO_2 before and after photocatalysis, (c) bond energies of the Ag 3d doublets of silver-clay before and after photocatalysis and (d) Ag 3d doublets of Ag-clay/TiO_2 before and after photocatalysis.

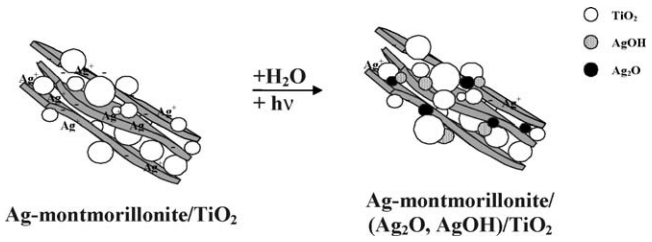

Fig. 3. The surface migration mechanism of Ag^+ ions in the presence of water vapour to the TiO_2 surface.

towards the lower energy range is observed (Ag-clay/TiO_2 E_b = 458.3 eV). The position of the Ti $2p_{3/2}$ component (458.7 eV) corresponds to the oxidation state of +4 of titanium dioxide [12,31].

In the case of the Ag-clay/TiO_2 composite (Fig. 2b), the binding energy of the oxygen derived from TiO_2 is modified from E_b = 531.07 eV to 531.74 eV by irradiation during photocatalysis and its intensity is reduced; in contrast, the energy of the oxygen peak associated with montmorillonite (E_b = 534.19 eV) is only slightly shifted (by ~0.1 eV) towards the higher bond energy range and its intensity is only minutely increased.

The binding energies of the Ag 3d doublets of silver-containing montmorillonite samples (E_b = 375.04 eV and E_b = 369.09 eV) are not modified by irradiation (Fig. 2c). The difference between the spin energies of the two peaks was measured as 6 eV, in good agreement with the results of Yang et al. [15]. After the addition of TiO_2 (Fig. 2d) the peaks cease to be symmetrical and a low-intensity shoulder appears, which is decreased by irradiation. Moreover, after the addition of TiO_2 the spectrum is shifted towards the lower energy range by ~1.5 eV, indicating that two new states of silver have appeared, of which the appearance of the peak with higher intensity (E_b = 367.5 eV) is attributable to the formation of silver oxide [32].

To sum up, bond energies are shifted in silver ion-exchanged composites in the course of irradiation during photocatalysis, which is due to the chemical reactions taking place on the surface. Based on our XPS measurements, we propose the following hypothesis to explain the conversions taking place on the surface: according to our hypothesis (Fig. 3), during photocatalysis in the presence of water vapour a multimolecular water layer is formed on the surface of the layer silicates, which makes possible the migration of silver ions on the adsorption layer, on the surface of the support, thus the resulting system contains both silver oxide and silver hydroxide. We suppose a surface reaction: $2Ag^+ + H_2O \rightarrow 2Ag_2O + 2H$-montm. or $Ag^+ + H_2O \rightarrow AgOH + H$-montm. occurs in contact with the TiO_2 catalyst. A detailed verification of these surface migration mechanisms, however, will necessitate further XPS and catalytic measurements.

3.4. Photocatalytic efficiency

The photocatalytic efficiency of ion-exchanged composites was tested in ethanol oxidation at a relative humidity of 70%. The reference catalyst thin film was pure TiO_2 P25. The degradations were also carried out without catalyst with both light sources; ethanol concentration did not decrease in either case, which means that no self-photolysis takes place in the system. In the course of the measurements the decrease in ethanol concentration and the extent of carbon dioxide production were monitored (Figs. 4a, b and 5a, b). The reference chosen for the determination of the synergistic effect of the catalyst thin films was the decrease in ethanol concentration (Δc_{EtOH}) produced by pure TiO_2 (P25) in 10 min. Since composites with TiO_2 contents of 35%, 50%, 65% and 80% were prepared, the reference value was corrected according to

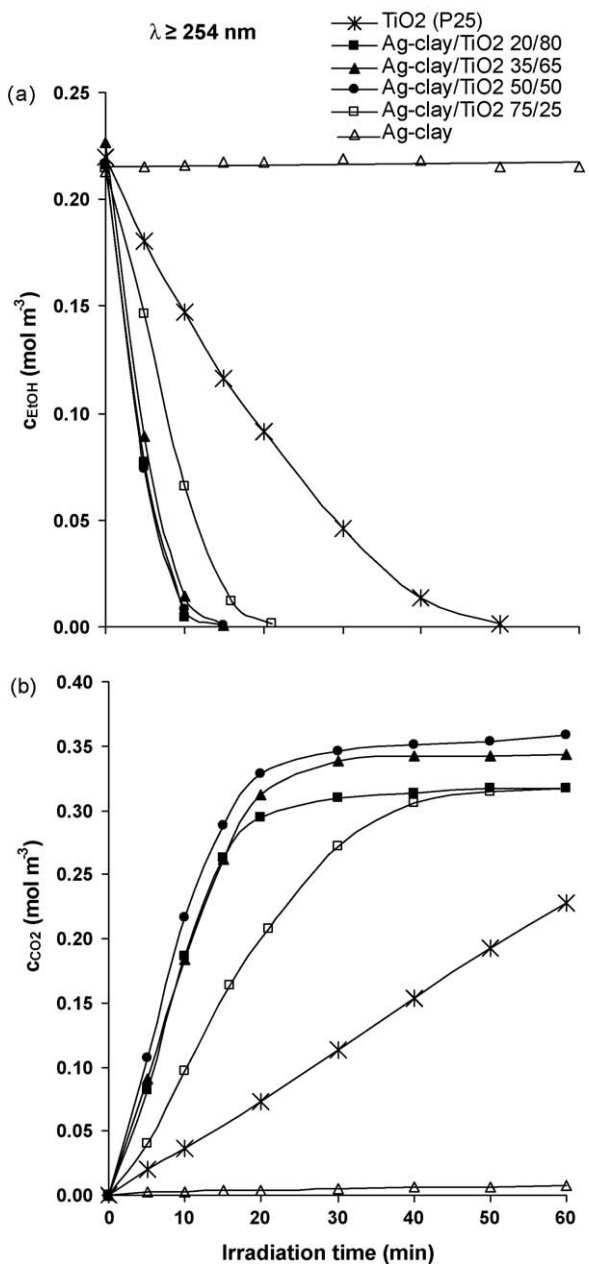

Fig. 4. (a) Changes of ethanol concentration under UV–vis irradiation (light source 1) and (b) formation of CO_2 as a function of irradiation time.

the different TiO_2 contents (w_1) of the composites. The synergistic effect can be calculated by the following the following equation:

$$\text{synergistic effect} = \frac{\Delta c_{(\text{EtOH})\text{Ag-clay/TiO}_2(\text{measured})}}{w_1\, \Delta c_{(\text{EtOH})\text{TiO}_2}} \times 100 \qquad (1)$$

where $\Delta c_{(EtOH)Ag-clay/TiO_2}$ is the decrease in ethanol concentration produced by the Ag-clay/TiO_2 composites in 10 min, and $w_1\, \Delta c_{(EtOH)TiO_2}$ is the decrease in ethanol concentration in 10 min based on the mass ratio (w_1) of pure TiO_2 photocatalyst. The data are shown in Figs. 4–6.

Inspection of the degradation curves (Fig. 4a and b) reveals that under $\lambda \geq 254$ nm irradiation the reference material, TiO_2 P25 does not degrade the entire amount of ethanol present in the reaction system even in 60 min, whereas the Ag-montm./TiO_2 composite catalysts degrade the entire amount within less than 20 min. Comparison of the values measured to the data of the photo-

oxidative degradation of ethanol calculated from the results of measurements on pure TiO_2 film (Fig. 6a) reveals the synergistic effect of silver-montmorillonite, i.e. an approximately five- to sixfold increase in efficiency relative to the calculated value in the case of the Ag-montm./TiO_2 composites of 20/80, 35/65 and 50/50 ratios.

Under irradiation in visible range ($\lambda \geq 435$ nm), according to the evidence of the degradation curves on Fig. 5a the degradation of ethanol Δc_{EtOH} is 0.1 mol m^{-3} in the flow system by the reference material TiO_2 P25. For silver-containing composites, the degree of photooxidation is higher in the case of Ag-montm./TiO_2 20/80 sample (Δc_{EtOH} = 0.18 mol m^{-3}). The same results can be seen in Fig. 5b for the CO_2 formation on different catalyst composites. It is important to mention that under 60 min experiment the photodegradation of ethanol is not completed, because we have intermedier products showing the gas chromatograms. The

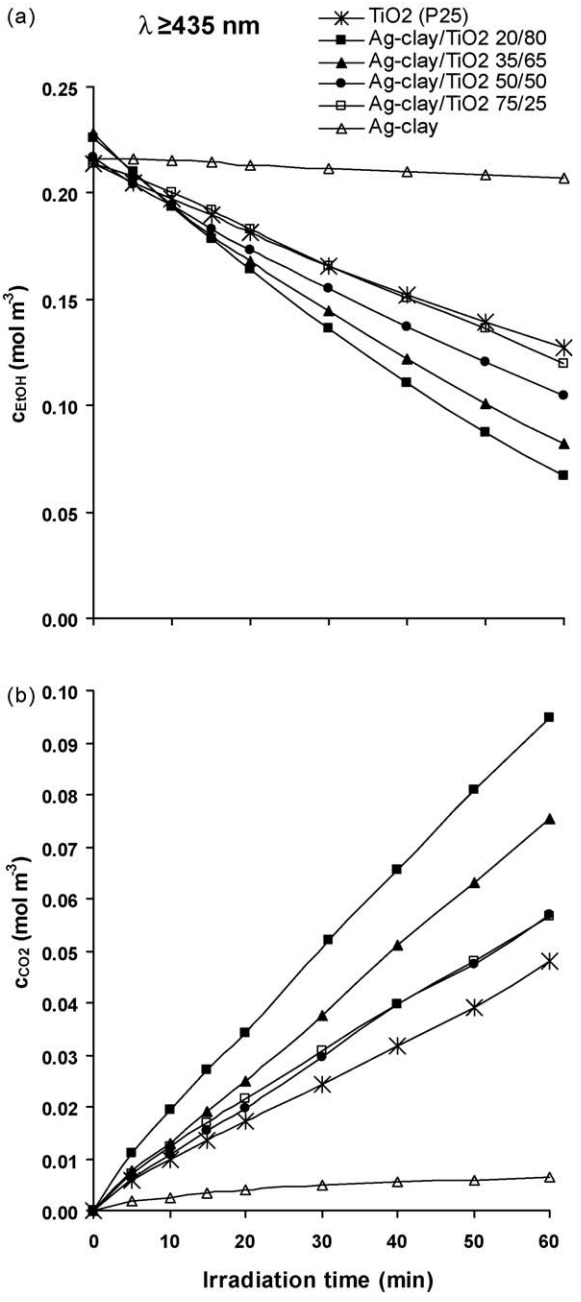

Fig. 5. (a) Changes of ethanol concentration under visible irradiation (light source 2) and (b) formation of CO_2 as a function of irradiation time.

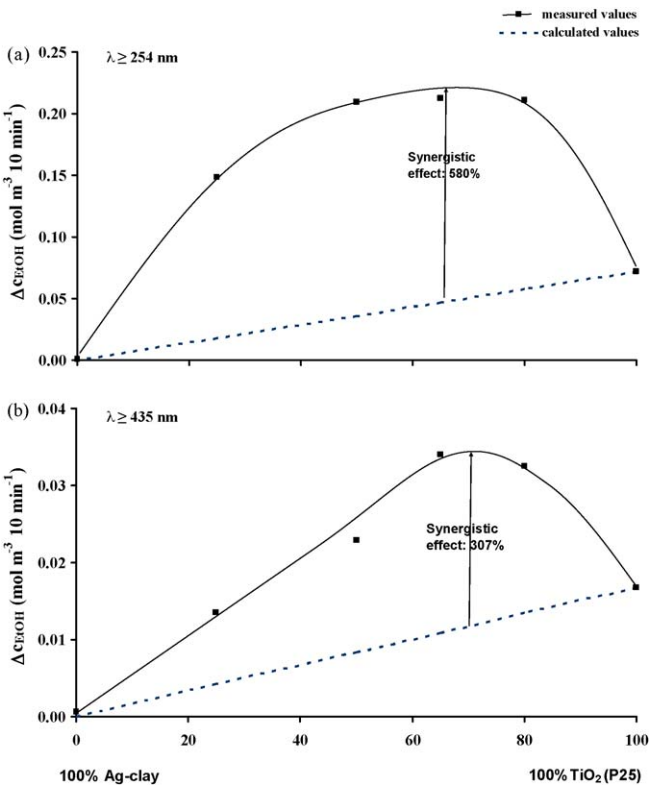

Fig. 6. The measured and calculated Δc_{EtOH} as a function of Ag-clay/TiO_2 composition under (a) UV–vis and (b) visible irradiation.

representation of the synergistic effect (Fig. 6a and b) reveals that the actual efficiency of the composites are much higher as the efficiency calculated for simple addition of TiO_2 and silver-clay content due to the presence of Ag-clay/TiO_2 composite sample.

To summarize our findings, it can be established that silver-montmorillonite has no significant photoactivity, since the initial amount of ethanol is not decreased after 1 h of UV irradiation. Ethanol is degraded more efficiently under UV-C irradiation ($\lambda \geq 254$ nm) than under visible light ($\lambda \geq 435$ nm) by each of the catalysts tested. The efficiency of photooxidative degradation by the various composites is significantly higher than the efficiency of the pure TiO_2 catalyst. The synergistic effect is due, on the one hand, to the excellent adsorption capability of the clay mineral for adsorbing ethanol, and on the other hand, to an increase in light quantum efficiency brought about by adding with silver ions into the clay/TiO_2 composite, caused by increased photon absorption in the λ = 450–650 nm wavelength.

4. Conclusion

Sodium-montmorillonite was exchanged with silver ions and the silver-montmorillonite was used for the preparation of various composites with TiO_2. The composites exhibiting novel optical properties were characterized by DR-UV–vis spectrophotometry. The energies of the samples were determined (λ_g exchanged from 387 nm to 402 nm) and it was shown that photon absorption maximum of the catalyst in the visible range (450–650 nm) is significantly increased by the incorporation of silver into the composites.

XPS measurements suggest that silver oxide and silver hydroxide nanoparticles modify the surface of TiO_2. The detailed verification of these surface migration mechanisms, however, necessitate further surface chemical studies. Thin composite films were prepared, whose photocatalytic properties were tested in the

degradation of ethanol vapour on the solid/gas interface, at a relative humidity of 70%. The efficiency of ethanol degradation was much higher under UV-C irradiation than in visible light for each catalyst and catalyst composite. The efficiency of the Ag-clay/TiO_2 composite with a mixing ratio of 20/80 was five- to sixfold higher than that of pure TiO_2.

References

[1] N.A. Kotov, I. Dekany, J.H. Fendler, Journal of Physical Chemistry 99 (1995) 13065–13069.
[2] M. Addamo, V. Augugliaro, A. Di Paola, E. García-López, V. Loddo, G. Marcí, L. Palmisano, Thin Solid Films 516 (2008) 3802–3807.
[3] P. Billik, G. Plesch, V. Brezová, L. Kuchta, M. Valko, M. Mazúr, Journal of Physics and Chemistry of Solids 68 (2007) 1112–1116.
[4] M. Addamo, V. Augugliaro, S. Coluccia, M.G. Faga, E. García-López, V. Loddo, G. Marcí, G. Martra, L. Palmisano, Journal of Catalysis 235 (2005) 209–220.
[5] J. Tschirch, D. Bahnemann, M. Wark, J. Rathousky, Journal of Photochemistry and Photobiology A: Chemistry 194 (2008) 181–188.
[6] V.A. Sakkas, P. Calza, C. Medana, A.E. Villioti, C. Baiocchi, E. Pelizzetti, T. Albanis, Applied Catalysis B: Environmental 77 (2007) 135–144.
[7] C. Sahoo, A.K. Gupta, A. Pal, Dyes and Pigments 66 (2005) 189–196.
[8] V. Augugliaro, H. Kisch, V. Loddo, M.J. López-Munoz, C. Márquez-Álvarez, G. Palmisano, L. Palmisano, F. Parrino, S. Yurdakal, Applied Catalysis A: General 349 (2008) 182–188.
[9] V.N. Kuznetsov, N. Serpone, Journal of Physical Chemistry C 111 (2007) 15277–15288.
[10] N. Serpone, Journal of Physical Chemistry B 110 (2006) 24287–24293.
[11] M. Anpo, M. Takeuchi, Journal of Catalysis 216 (2003) 505–506.
[12] L. Kőrösi, Sz. Papp, J. Ménesi, E. Illés, V. Zöllmer, A. Richardt, I. Dékány, Colloids and Surfaces A 319 (2008) 136–142.
[13] M. Bellardita, M. Addamo, A. Di Paola, L. Palmisano, Chemical Physics 339 (2007) 94–103.
[14] C.C. Chang, J.Y. Chen, T.L. Hsu, C.K. Lin, C.C. Chan, Thin Solid Films 516 (2008) 1743–1747.
[15] X. Yang, L. Xu, X. Yu, Y. Guo, Catalysis Communications 9 (2008) 1224–1229.
[16] H.E. Chao, Y.U. Yun, H.U. Xingfang, A. Larbot, Journal of the European Ceramic Society 23 (2003) 1457–1464.
[17] D.B. Hamal, K.J. Klabunde, Journal of Colloid and Interface Science 311 (2007) 514–522.
[18] M.K. Seery, R. George, P. Floris, S.C. Pillai, Journal of Photochemistry and Photobiology A 189 (2007) 258–263.
[19] C. He, Y. Yu, X. Hu, A. Larbot, Applied Surface Science 200 (2002) 239–247.
[20] W. Wang, J. Zhang, F. Chen, D. He, M. Anpo, Journal of Colloid and Interface Science 323 (2008) 182–186.
[21] J. Arfaoui, L. Khalfallah Boudali, A. Ghorbel, G. Delahay, Journal of Physics and Chemistry of Solids 69 (2008) 1121–1124.
[22] J. Ménesi, L. Kőrösi, É. Bazsó, V. Zöllmer, A. Richardt, I. Dékány, Chemosphere 70 (2008) 538–542.
[23] I. Ilisz, A. Dombi, K. Mogyorósi, I. Dékány, Applied Catalysis B: Environmental 39 (3) (2002) 247–256.
[24] R. Kun, K. Mogyorósi, I. Dékány, Applied Clay Science 32 (2006) 99–110.
[25] S. Sun, Y. Jiang, L. Yu, F. Li, Z. Yang, T. Hou, D. Hu, M. Xia, Materials Chemistry and Physics 98 (2006) 377–381.
[26] G. Zhang, X. Ding, F. He, X. Yu, J. Zhou, Y. Hu, J. Xie, Journal of Physics and Chemistry of Solids 69 (2008) 1102–1106.
[27] J. Liu, X. Li, S. Zou, Y. Yu, Applied Clay Science 37 (2007) 275–280.
[28] J. Ménesi, R. Kékesi, L. Kőrösi, V. Zöllmer, A. Richardt, I. Dékány, International Journal of Photoenergy (2008) (Article ID 846304).
[29] L. Kőrösi, A. Oszkó, G. Galbács, A. Richardt, V. Zöllmer, I. Dékány, Applied Catalysis B: Environmental 129 (2007) 175–183.
[30] E.P. Barrett, L.G. Joyner, P.P. Halenda, Journal of the American Chemical Society 73 (1951) 373–380.
[31] F. Zhang, G.K. Wolf, X. Wang, X. Liu, Surface & Coatings Technology 148 (2001) 65–70.
[32] S.M. Magana, P. Quintana, D.H. Aguilar, J.A. Toledo, C. Ángeles-Chávez, M.A. Cortés, L. León, Y. Freile-Pelegrín, T. López, R.M. Torres Sánchez, Journal of Molecular Catalysis A 281 (2008) 192–199.
[33] I. Dékány, F. Szántó, L.G. Nagy, Colloid and Polymer Science 266 (1988) 405–417.